Inorganic Chemistry
Article

Inorg. Chem. **2010**, *49*, 11473–11484 **11473**
DOI: 10.1021/ic101547r

Non-Centrosymmetric Tetrameric Assemblies of Tetramethylammonium Halides with Uranyl Salophen Complexes in the Solid State

Massimo Cametti,*,†,§ Laura Ilander,† Arto Valkonen,†,∥ Martin Nieger,‡,∥ Maija Nissinen,†,⊥ Elisa Nauha,†,⊥ and Kari Rissanen*,†

†*Department of Chemistry, Nanoscience Center, University of Jyväskylä, FIN-40014 JYU, Finland, and* ‡*Department of Chemistry, Laboratory of Inorganic Chemistry, University of Helsinki, Helsinki, Finland.* §*Present address: NFMLab, Dipartimento di Chimica, Materiali ed Ingegneria Chimica,"Giulio Natta", Politecnico di Milano, Via L. Mancinelli 7, 20131 Milan, Italy.* ∥*Data collection, structure solution and refinement of* ***6****, 7-(TMA)Cl, 7-(TMA)F, and* ***8****.* ⊥*Data collection, structure solution and refinement of* ***3****-(TMA)Cl and* ***4****-(TMA)F*

Received August 1, 2010

Ditopic salophen-UO_2 receptors **1**−**4** and **7** co-crystallize with tetramethylammonium (TMA) chloride and fluoride salts producing good quality crystals amenable for X-ray diffraction characterization. The arrangement of the receptor and salt units in the crystal lattice is such that tetrameric ball-shaped assemblies are formed, where an inner cluster of four TMA cations are surrounded by an outer shell of four UO_2-bound anions. These elaborate architectures, which occur in all cases, regardless of a certain degree of structural modification on the receptors, lead to lattices that belong to non-centrosymmetric (NCS) space groups. Interestingly, the tetragonal symmetry of the tetrameric ball-shaped assemblies is either retained ($I\bar{4}$) or lost ($R3c$ and $I\bar{4}3d$) at the lattice level, without compromising the NCS nature of the crystal lattices. The principal X-ray investigation on TMAX (X=Cl/F) co-crystals, that is, **1**-(TMA)Cl, **2**-(TMA)Cl, **3**-(TMA)Cl, **4**-(TMA)Cl, **7**-(TMA)Cl, and **7**-(TMA)F, is accompanied by NMR and electrospray ionization (ESI) mass spectrometry studies to gather additional insight on the modality of formation of the solid state structures observed. The important role of cation-π interactions in the receptor-salt recognition process is renewed and strengthened by comparison with NMR titration data with a novel reference compound, the salophen-UO_2 complex **8**. Given the importance of NCS and polar crystalline solids in the development of functional materials, this study shows that this property can be introduced into elaborate host−guest systems, as those which assemble in the architectures described here, thus expanding its field of applicability.

Introduction

Material chemistry is a central topic in modern science.[1] Among the many features which materials possess, the symmetry elements present in the crystal lattice have a crucial effect in determining the material properties. Whenever in a given crystalline material the molecular components are ordered so that they do not show a center of inversion, namely, in a non-centrosymmetric lattice, a series of interesting properties, such as pyro-, ferro-, and piezo-electricity, may occur.[2] Non-centrosymmetric (NCS) space groups are the majority, 21 over the 32 crystallographic point groups lack of a center of symmetry,[3] and they include chiral and polar space groups as subcategories. Indeed, for the sake of clarity, it must be stressed that not all the NCS space groups are polar, although in the literature controversy on the term polar is quite frequently encountered.[4] Despite the large number of NSC crystal structures reported in the literature,

*To whom correspondence should be addressed. E-mail: massimo.cametti@gmail.com (M.C.); kari.t.rissanen@jyu.fi (K.R.).

(1) *Functional Organic Materials*; Müller, T. J. J., Bunz, U. H. F., Eds.; Wiley-VCH Verlag GmbH & Co.: Weinheim, Germany, 2007; Cullity, B. D.; Graham, C. D. *Introduction to Magnetic Materials*; Institute of Electrical and Electronics Engineers, Inc.: New York, 2009; *Nano-Architectured and Nanostructured Materials*; Champion, Y., Fecht, H.-J., Eds.; Wiley-VCH Verlag GmbH & Co.: Weinheim, Germany, 2004; *The Supramolecular Chemistry of Organic-Inorganic Hybrid Materials*; Rurack, K., Martínez-Máñez, K., Eds.; John Wiley & Sons, Inc.: New York, 2010.

(2) Horiuchi, S.; Tokunaga, Y.; Giovannetti, G.; Picozzi, S.; Itoh, H.; Shimano, R.; Kumai, R.; Tokura, Y. *Nature* **2010**, *463*, 789–792. Chang, H. Y.; Sivakumar, T.; Ok, K. M.; Halasyamani, P. S. *Inorg. Chem.* **2008**, *47*, 8511–8517. Ok, K. M.; Chi, E. O.; Halasyamani, P. S. *Chem. Soc. Rev.* **2006**, *35*, 710–717. Hollingsworth, M. D. *Science* **2002**, *295*, 2410–2413. Halasyamani, P. S.; Poeppelmeier, K. R. *Chem. Mater.* **1998**, *10*, 2753. Nye, J. F. *Physical Properties of Crystals*; Clarendon Press: Oxford, U.K., 1985.

(3) Pidcock, E. *Chem. Commun.* **2005**, 3457–3459. Curtin, D. Y.; Paul, I. C. *Chem. Rev.* **1981**, *81*, 525–541.

(4) (a) Bomfin, J. A. S.; Filgueiras, C. A. L.; Alan Howie, R.; Low, J. N.; Skakle, J. M. S.; Wardell, J. L.; Wardell, S. M. S. V. *Polyhedron* **2002**, *21*, 1667–1676. (b) Cieslinski, M.; Steel, P. J.; Lincoln, S. F.; Easton, C. J. *Supramol. Chem.* **2006**, *18*, 529–536. (c) Kiviniemi, S.; Sillanpää, A.; Nissinen, M.; Rissanen, K.; Lämsä, M. T.; Pursiainen, J. *Chem. Commun.* **1999**, 897–898.

Published on Web 11/23/2010

Scheme 1. Molecular Formulae for the Uranyl Salophen Complexes **1**−**8**

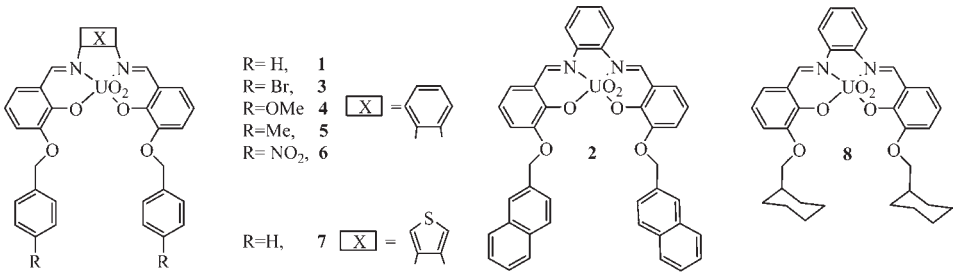

the knowledge acquired so far is not sufficient to predict, with rare exceptions,[5] whether or not a given species will produce a NCS crystal structure, especially when dealing with achiral molecules.

Both experimental and computational studies aimed to gather data on structure-properties relationships mainly focus on simple molecules that are easily modified and tractable.[6] However, although less common, NCS and polar materials can be obtained by more elaborate packing motifs,[7] especially when the molecular components have a tendency to self-assemble into complex architectures.[4c,7d]

In the course of our studies on ditopic receptors we have established a family of uranyl salophen complexes as efficient binders for several classes of organic and inorganic ion pairs.[8] In particular, we have demonstrated that receptors **1** and **2** (Scheme 1) bind hard halides via coordination with the UO_2 center, and, at the same time, they make use of the two adjunct aromatic side arms to further stabilize, via cation-π interactions, the tertiary receptor-anion-cation adducts. Such ternary complexes for tetramethylammonium (TMA) chloride were characterized by X-ray diffraction on single crystals grown by slow evaporation solution of **1** and **2** in the presence of (TMA)Cl, as described in (our) previous communications.[8a,c]

An intriguing feature of the solid state complexes of (TMA)Cl with **1** and **2** is provided by their particular organization of the receptors and of the salt units to form tetrameric ball-shaped assemblies, $[(TMA)_4]@[(Cl\text{-}\mathbf{1})_4]$ and $[(TMA)_4]@[(Cl\text{-}\mathbf{2})_4]$, constituted of an inner cluster of four TMA cations surrounded by an outer layer of four chloride-uranyl salophen complexes. These tetramers are further arranged into a lattice devoid of any center of inversion and thus crystallize in NCS space groups ($I\bar{4}$ and $R3c$). At variance with simpler and more common cases, the repeating unit is constituted by the compact tetrameric assembly of defined geometry composed of eight molecular species (four receptors and four ion pairs).

Notably, very different behavior has been observed when the TMA cation was replaced with tetrabutylammonium (TBA). The large size of the TBA cation prevents the formation of the closed shell-like structure specific to the small TMA and instead leads to a columnar staking of alternate cation/UO_2-anion units.[8a]

Given the scarcity of similarly structurally complex cases, we set out on a detailed structural study of these systems and of newly synthesized derivatives.

With this in mind, uranyl salophens **3**−**6** (Scheme 1), bearing a series of different substituents, were synthesized (see Experimental Section) in order verify the amount of structural modification that such structures could endure without significantly altering the nature of the crystal lattice. Complex **7** (Scheme 1), in which the upper benzenoid ring is replaced with the heterocyclic thiophene moiety, was also synthesized for comparison.

The crystal structures of **1** and **2** with (TMA)Cl were obtained in previous investigations.[8a,c] We were able to obtain good quality single crystals of the **3-**, **4-**, and **7-**(TMA)Cl complexes, and of **7-**(TMA)F complex. Co-crystallization of receptors **5** and **6** with (TMA)Cl, under the same conditions, failed to produce the desired complexes. However, the crystal structure of the *solvated* receptor **6** was also obtained.

The importance of cation-π interactions in such systems is well documented.[8] To gain more insight on the overall contribution of cation-π interactions on the process of formation of the tetrameric aggregates, compound **8** (Scheme 1), which lacks of aromatic side arms and is decorated with cyclohexyl moieties instead, was studied by ^{1}H NMR and electrospray ionization (ESI) mass spectrometry. This allowed to assess its binding affinity to (TMA)Cl in solution and in the gas phase, in direct comparison with **1**. The solid state structure of *solvated* receptor **8** is also reported.

Experimental Section

2-Allyloxy-3-hydroxy-benzaldehyde. Synthesis already described in *J. Am. Chem. Soc.* **1988**, *110*, 4992.

General Procedure for the Syntheses of Aldehydes 9−11 and 13. To a suspension of NaH (0.022 mol, 60% in oil), prewashed with *n*-pentane, in dimethylsulfoxide (DMSO, 10 mL), was added dropwise a solution of 2,3-dihydroxybenzaldehyde (1.5 g, 0.01 mol) in DMSO (5 mL) at 20−25 °C, under N_2 atmosphere. After 1 h of stirring, a solution of the proper *p*-substituted benzyl bromide (or chloromethyl-cyclohexane) (0.01 mol) in DMSO (25 mL) was added at 20−25 °C, and stirring was continued for 12−24 h, whereupon the mixture was poured into water (50 mL) and extracted with $CHC1_3$ (3 × 25 mL).

(5) Saha, B. K.; Nangia, A.; Nicoud, J.-F. *Cryst. Growth Des.* **2006**, *6*, 1278–1281. Glaser, R.; Knotts, N.; Wu, H. *Chemtracts: Org. Chem.* **2003**, *16*, 643–652. Holman, K. T.; Pivovar, A. M.; Ward, M. D. *Science* **2001**, *294*, 1907–1911. Anthony, S. P.; Radhakrishnan, T. P. *Chem. Commun.* **2001**, 931–932.

(6) Woitaś, M.; Gabor, A.; Czupiński, O.; Pietraszko, A.; Jakubas, R. *J. Solid State Chem.* **2009**, *182*, 3021–3030. Piana, S.; Reyhani, M.; Gale, J. D. *Nature* **2005**, *438*, 70–73. Hiremath, R.; Varney, S. W.; Swift, J. A. *Chem. Mater.* **2004**, *16*, 4948–4954. Hulliger, J.; Bebie, H.; Kluge, S.; Quintel, A. *Chem. Mater.* **2002**, *14*, 1523–1529. Hulliger, J.; Roth, S. W.; Quintel, A.; Bebie, H. J. *Solid State Chem.* **2000**, *152*, 49–56.

(7) (a) Muppidi, V. K.; Zacharias, P. S.; Pal, S. *J. Solid State Chem.* **2007**, *180*, 132–137. (b) Hang, T.; Fu, D.-W.; Ye, Q.; Xiong, R.-G. *Cryst. Growth Des.* **2009**, *9*, 2026–2029. (c) Sun, H.-L.; Ma, B.-Q.; Gao, S.; Batten, S. R. *Cryst. Growth Des.* **2006**, *6*, 1261–1263. (d) Lipstman, S.; Muniappan, S.; Goldberg, I. *Cryst. Growth Des.* **2008**, *8*, 1682–1688. (e) Seward, C.; Pang, J.; Wang, S. *Eur. J. Inorg. Chem.* **2002**, 1390–1399. (f) Thalladi, V. R.; Boese, R.; Brasselet, S.; Ledoux, I.; Zyss, J.; Jetti, R. K. R.; Desiraju, G. R. *Chem. Commun.* **1999**, 1639–1640.

(8) (a) Cametti, M.; Nissinen, M.; Dalla Cort, A.; Mandolini, L.; Rissanen, K. *Chem. Commun.* **2003**, 2420–2421. (b) Cametti, M.; Nissinen, M.; Dalla Cort, A.; Mandolini, L.; Rissanen, K. *J. Am. Chem. Soc.* **2005**, *127*, 3831–3837. (c) Cametti, M.; Nissinen, M.; Dalla Cort, A.; Mandolini, L.; Rissanen, K. *J. Am. Chem. Soc.* **2007**, *129*, 3641–3648.

Scheme 2. Synthesis for the Aldehydes **9**−**13** and for the Salophen-UO_2 Complexes **3**−**8**[a]

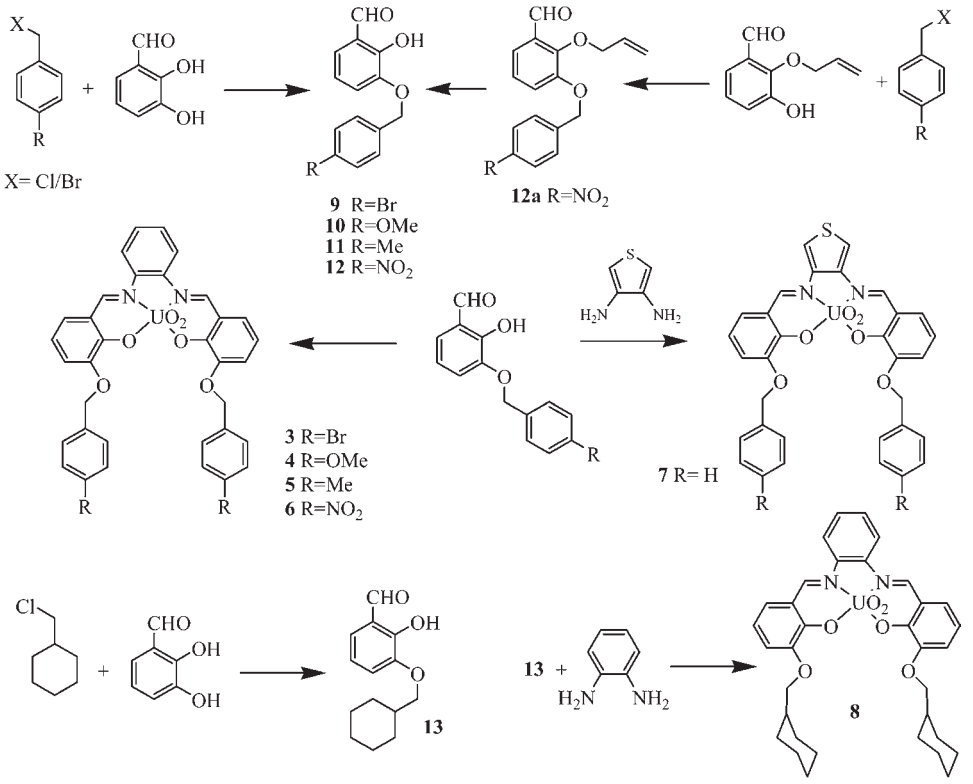

[a]Receptors **1** and **2** (Scheme 1) have been previously described.[8]

The aqueous layer was acidified with 6 M HCl to adjust the pH to 2−4, and it was again extracted with $CHC1_3$ (3×50 mL). The latter combined $CHC1_3$ layers were washed with 1 M HCl (2× 50 mL), concentrated and filtered over silica gel ($CHCl_3$) to give pure aldehydes **9**−**11** as a yellow solid (Scheme 2).

9: Yield: 78%, ^{1}H NMR ($CDC1_3$, 250 MHz): δ 11.06 (s, 1H, −OH), δ 9.89 (s, 1H, CHO), δ 7.37−7.15 (m, 6H), δ 6.94 (t, 1H), δ 5.56 (s, 2H, CH_2−O), ^{13}C NMR ($CHCl_3$, 63 MHz): δ 194.5, 161.5, 153.6, 147.2, 139.4, 134.5, 131.5, 129.3, 127.9, 122.3, 120.6, 72.0. Mass spectrum (EI), *m*/*z* 307 (M^+, calcd for $C_{14}H_{11}BrO_3$ 307.14). Elemental analysis: calcd for $C_{14}H_{11}BrO_3$, C 54.75, H 3.61; found: C 55.63, H 3.95.

10: yield 42%. Mp. 127.9 C°. ^{1}H NMR ($CDC1_3$, 250 MHz): δ 11.07 (s, 1H, −OH), δ 9.91 (s, 1H, CHO), δ 7.38−6.85 (m, 7H), δ 5.11 (s, 2H), δ 3.80 (s, 3H, CH_3O−). ^{13}C NMR (CDCl3, 63 MHz): δ 193.5, 159.9, 151.9, 148.0, 130.4, 129.5, 123.5, 121.8, 120.6, 120.1, 114.7, 70.8, 55.9. Mass spectrum (EI): *m*/*z* 258 (M^+, calcd for $C_{15}H_{14}O_4$ 258.27). Elemental analysis: calcd for $C_{15}H_{14}O_4$, C, 69.76; H, 5.46; found: C 71.2, H 5.98.

11: yield 75%; ^{1}H NMR ($CDC1_3$, 250 MHz): δ 11.02 (s, 1H, −OH), δ 9.91 (s, 1H, CHO), δ 7.35−7.11 (m, 6H), δ 6.89 (t, 1H), δ 5.51 (s, 2H, CH_2−O), δ 2.35 (s, 3H, CH_3-). ^{13}C NMR (CDCl3, 63 MHz): δ 196.6, 152.5, 147.4, 138.1, 133.7, 129.5, 127.7, 125.4, 121.3, 119.6, 71.6, 21.4. Mass spectrum (EI), *m*/*z* 242 (M^+, calcd for $C_{15}H_{14}O_3$ 242.27). Elemental analysis: calcd for $C_{15}H_{14}O_3$, C, 74.36; H, 5.82; found: C 75.41, H 6.23.

12a: 2-Allyloxy-3-hydroxy-benzaldehyde (0.5 g) is dissolved in CH_3CN (15 mL), and K_2CO_3 is added (0.65 g). After 30 min a solution 0.73 g of *p*-nitrobenzyl bromide in CH_3CN (5 mL) is added. After 6 h no starting products are detectable on TLC, and 50 mL of water are added. The solution is extracted with $CHCl_3$ (4×30 mL), and the combined organic layers are washed with water (2× 50 mL) and dried with Na_2SO_4. The solvent is then evaporated in vacuo. Column SiO2/($CHCl_3$:cyclohexane 25%)→$CHCl_3$) afforded the desired product. Yield: 83%. ^{1}H NMR ($CDCl_3$): δ 10.44 (s, 1H, CHO); δ 8.27 (2H, d, *J* = 8.5 Hz), δ 7.63 (2H, d, 8.5 Hz), δ 7.49−7.11 (3H, m), δ 6.078 (1H, m), δ 5.34 (2H, m), δ 5.24 (2H, s), δ 4.68 (2H, d, 6 Hz); ^{13}C (DMSO-d6, 63 MHz): δ 192.357, 150.859, 147.045, 146.794, 144.642, 139.78, 128.252, 123.506, 122.868, 121.329, 119.551, 119.234, 116.76 69.031, 63.65; Mass spectrum (EI), *m*/*z* 313 (M^+, calcd for $C_{17}H_{15}NO_5$ 313.1). Elem. analysis: calcd for $C_{17}H_{15}NO_5$ C, 65.17; H, 4.83; N, 4.47; found: C 66.23, H 5.23, N 4.23.

12: A 1 g portion of **12a** is added with 350 mg of SeO_2 and 180 mg of acetic acid in dioxane (35 mL). The solution is refluxed for 3 h, then 50 mL of water is added. The solution is extracted with CH_2Cl_2 and the organic phase dried over Na2SO4. Column SiO_2,CH_2Cl_2/cyclohexane(20%)→CH_2Cl_2/acetone (10%). Yield: 85%. ^{1}H NMR (DMSO-d6, 250 MHz): δ 10.45 (1H, s), δ 10.27 (1H, s); δ 8.26 (2H, d, *J* = 8.75 Hz), δ 7.78 (2H, d, *J* = 8.75 Hz) δ 7.3 (2H, m)); δ 6.90 (1H, t, 8 Hz), δ 5.37 (2H, s); Mass spectrum (EI), *m*/*z* 273 (M^+, calcd for $C_{14}H_{11}NO_5$ 273.24); ^{13}C NMR (DMSO-d6, 63 MHz): δ 192.4, 150.8, 147.0, 146.8, 144.6, 128.2, 123.5, 122.9, 121.3, 119.5, 119.2, 69.0; Elemental analysis: calcd for $C_{14}H_{11}NO_5$ C, 61.54; H, 4.06; N, 5.13; found: C 62.42, H 4.98, N 4.89.

13: yield 65%; ^{1}H NMR (DMSO-d6, 250 MHz): δ 10.24 (1H, s), δ 10.09 (1H, s, broad), δ 7.22 (2H, d, *J* = 7.5 Hz), δ 6.89 (1H, t, *J* = 7.5 Hz), δ 3.83 (2H, d, *J* = 6.2 Hz), 1.78 (6H, m), 1.1 (5H, m); ^{13}C NMR (DMSO, 63 MHz): δ 192.6, 150.7, 147.7, 122.4, 120.5, 119.2, 118.6, 73.9, 36.9, 29.1, 26.0, 25.2; Mass spectrum (EI), *m*/*z* 234 (M^+, calcd for $C_{14}H_{18}O_3$ 234.13). Elemental analysis: calcd for $C_{14}H_{18}O_3$ C, 71.77; H, 7.74; found: C 70.25, H 7.89.

General Procedure for the Synthesis of Receptors 3−8. To a refluxing solution of **9**−**12** (3 mmol) in methanol (70 mL) is added dropwise a solution of 1,2-benzenediamine (or 3,4-diaminothiophene) (1.5 mmol) in MeOH (25 mL). After 1.5 h $UO_2(OAc)_2\cdot 2H_2O$ (1.5 mmol) is added and reflux is maintained for 15−30 min. The mixture is allowed to cool to room temperature overnight. The red solid formed is filtered and dried in

vacuo. Purification by column chromatography (SiO_2/$CHCl_3$ or $CHCl_3$:acetone 9:1) is performed in cases where simple crystallization from methanol does not yield the pure compound.

3: Yield 50%, ^{1}H NMR (DMSO-d6, 250 MHz): δ 9.59 (s 2H, CH=N), δ 8.13−7.36 (m, 16H), δ 6.62 (t, 2H), δ 5.33 (s, 4H). ^{13}C NMR (DMSO-d6, 63 MHz): δ 169.2, 160.87, 149.6, 149.3, 138.7, 128.4, 127.7, 127.2, 126.1, 125.3, 123.4, 122.4, 119.7, 111.4, 74.3 ppm; Mass spectrum (ESI): m/z 977.27 ([M+Na]$^+$, calcd for $C_{34}H_{24}O_6N_2UBr_2Na$ 977.4); Elemental analysis: calcd for $C_{34}H_{24}O_6N_2UBr_2$ C 42.79, H 2.53, N 2.94; found C 42.12, H 2.76, N 3.01.

4: Yield 56%, ^{1}H NMR (CD_3OD, 250 MHz): δ 9.64 (s, 2H, CH=N), δ 7.76−7.02 (m, 16H), δ 6.74 (t, 2H), δ 5.32 (s, 4H, CH_2−O), δ 3.88 (s, 6H, CH_3O−); ^{13}C NMR (CD_3OD, 63 MHz): δ 167.5, 160.9, 150.3, 145.6, 137.9, 135.4, 128.5, 128.1, 127.9, 126.8, 124.3, 121.8, 119.5, 112.7, 72.6, 57.3 ppm; Mass spectrum (ESI), m/z 857.45 ([M+H]$^+$, calcd for $C_{36}H_{30}O_8N_2U$ 857.66); Elemental analysis: calcd for $C_{36}H_{30}O_8N_2U$ C 50.47, H 3.53, N 3.27), found C 50.30, H 3.74, N 3.11.

5: Yield 50%, ^{1}H NMR (DMSO-d6, 250 MHz): δ 9.61 (s 2H, CH=N), δ 8.13−7.34 (m, 16H), δ 6.59 (t, 1H), δ 5.30 (s, 4H), δ 2.33 (s, 3H, CH_3-). ^{13}C NMR (DMSO-d6, 63 MHz): δ 166.2, 161.3, 149.7, 146.6, 136.7, 134.6, 128.7, 128.4, 127.9, 127.8, 124.4, 120.1, 119.9, 115.6, 70.5, 20.5 ppm; Mass spectrum (ESI), m/z 847.45 ([M+Na]$^+$, calcd for $C_{36}H_{30}O_6N_2UNa$ 847.66); Elemental analysis: calcd for $C_{36}H_{30}O_6N_2U$ C 52.43, H 3.67, N 3.40; found: C 51.35, H 3.80, N 3.23.

6: Yield: 65%, ^{1}H NMR (DMSO-d6, 250 MHz): δ 9.64 (s, 2H), δ 8.28 (d, 4H, 8.5 Hz), δ 7.87 (d, 4H, 8.5 Hz), δ 7.76 (m, 2H), δ 7.55 (m, 2H), δ 7.47 (d, 2H, 7.5 Hz), δ 7.32 (d, 2H, 7.7 Hz), δ 6.61 (t, 2H, 7.6 Hz), δ 5.56 (s, 4H). ^{13}C (DMSO-d6, 63 MHz): δ 171.2, 161.7, 149.2, 146.4, 139.8, 132.2, 130.8, 127.8, 127.1, 126.4, 124.4, 123.0, 121.4, 115.4, 73.2 ppm; Mass spectrum (ESI), m/z 909.53 ([M+Na]$^+$, calcd for $C_{34}H_{24}N_4O_{10}UNa$ 909.6; Elemental analysis: calcd for $C_{34}H_{24}N_4O_{10}U$ C, 46.06; H, 2.73; N, 6.32; found: C 47.23, H 3.23, N 7.24.

7: Yield: 60%, ^{1}H NMR (DMSO-d6, 500 MHz,): δ 9.71 (s, 2H), δ 7.96 (s, 2H), δ 7.60 (d, 4H, J = 7.5 Hz), δ 7.43 (tt, 4H, J_1 = 1.5 Hz, J_2 = 7.6 Hz), δ 7.40 (dd, 2H, J_1 = 1.6 Hz, J_2 = 8.2 Hz), δ 7.36 (tt, 2H, J_1 = 1.3 Hz, J_2 = 2.2 Hz, J_3 = 7.4 Hz), δ 7.33 (dd, 2H, J_1 = 1.6 Hz, J_2 = 7.8 Hz), δ 6.63 ppm (t, 2H, J = 7.8 Hz); ^{13}C NMR (DMSO-d6, 126 MHz): δ 166.3, 161.3, 150.0, 147.9, 137.7, 128.5, 128.2, 127.9, 124.3, 122.9, 119.8, 116.1, 111.4, and 70.5 ppm; Mass spectrum (ESI): m/z calcd for $C_{33}H_{27}O_7N_2SU$ 833.7 [M+CH_3O]$^-$; found: 833.4; Elemental analysis: calcd. for $C_{32}H_{24}O_6N_2SU$: C, 47.88; H, 3.01; N, 3.49; O; found: C, 46.93; H, 3.24; N, 3.42.

8: Yield: 65%, ^{1}H NMR (DMSO-d6, 500 MHz): δ 9.59 (2H, s), δ 7.74−7.76 (2H, m), δ 7.52−7.54 (2H, m), δ 7.39 (2H, dd, J_1 = 1.5 Hz, J_2 = 8.1 Hz), δ 7.24 (2H, dd, J_1 = 1.5 Hz, J_2 = 7.7 Hz), δ 6.59 (2H, t, J = 7.8 Hz), δ 4.99 (4H, d, J = 7.0 Hz), δ 1.78−1.81 (4H, m), 1.70−1.73 (2H, m), δ 1.24−1.39 (8H, m), and δ 1.12−1.19 ppm (4H, m); ^{13}C NMR (DMSO-d6, 126 MHz): δ 166.4, 161.1, 150.4, 146.8, 128.6, 127.2, 124.2, 120.1, 118.7, 115.9, 74.0, 37.3, 29.5, 26.1, 25.3 ppm; Mass spectrum (ESI): m/z calcd. for $C_{35}H_{41}O_7N_2U$ 839.8 [M+CH_3O]$^-$; found: 839.5; Elemental analysis: calcd. for $C_{34}H_{38}O_6N_2U$+3 H_2O (M_r 862.796): C, 47.44; H, 4.92; N, 3.25. Found: C, 47.47; H, 4,79; N, 3.27.

X-ray Crystallography. Suitable single crystals for complexes **3-**, **4-**, and **7**-(TMA)Cl and **7**-(TMA)F were obtained from slow evaporation of a CH_2Cl_2/$CHCl_3$ solution of receptor with a 3−10 molar excess of (TMA)Cl. Single crystals for the solvates of receptors **6** and **8** were obtained by slow evaporation of a receptor solution in acetone/DMF and MeCN/$CHCl_3$, respectively. The X-ray diffraction analyses were performed using a Bruker-Nonius KappaCCD diffractometer equipped with Apex II detector and utilizing graphite-monochromatized Mo−K_α (λ = 0.71073 Å) radiation. Collect software[9] was used for the data measurement and DENZO-SMN[10] for the processing. Except for **4**-(TMA)Cl, all the structures were solved by direct methods with SIR97/SIR2004[11] and refined by full-matrix least-squares methods with WinGX-software,[12] which utilizes the SHELXL-97 module;[13a] **4**-(TMA)Cl was solved by SHELXS.[13b] All C−H hydrogen positions were calculated in the idealized positions by using a riding atom model after the anisotropic refinement of all non-hydrogen atoms of the structure. If possible, all N−H (or $^+$N−H) hydrogens were located from the electron density map and refined with restrained bond distances using isotropic displacement parameters of $1.2U_{eq}$ (or $1.5U_{eq}$) of the attached N-atom. Most of the O−H hydrogens were located from the electron density map and refined as a rotating group by using the same ($1.2U_{eq}$ or $1.5U_{eq}$) isotropic displacement parameters. Detailed crystallographic data for all structures are summarized in Table 1. In **4**-(TMA)Cl one of the methyl group of the receptor (C24) is disordered over two positions with fixed population parameter 0.5. Abs. corr. (SADABS2002 or 2008)[14] was applied to all structures except for **4**-(TMA)Cl where the absorption correction was applied but not used in the final refinement since it significantly reduced the quality the results.

NMR Studies. ^{1}H NMR spectra were recorded on a 250 MHz Bruker Advance spectrometer. Triphenylmethane was used as an internal standard. All ^{1}H NMR titrations were run at 25 °C according to a published procedure.[15] Each tested receptor was washed with $CHCl_3$ (amylene stabilized, three times) prior to the experiment.

ESI-MS Studies. ESI mass spectra were recorded on an LCT-TOF mass spectrometer with an electrospray ion source (Micromass LCT). Chloroform was used as spraying solvent in all experiments. Ionization parameters were adjusted as follows: capillary voltage: 3100 V; cone voltage: 20 V; sample cone: 5 V; RF lens: 1000 V. Desolvation and source temperatures were 120° and 80 °C, respectively. The S/N ratio was improved by scan average.

Results and Discussions

Salophen-UO_2 complex **1** and its derivatives **2**−**7** were originally designed as receptors for contact ion pairs. The UO_2-center is known to be capable of strong coordination to hard Lewis bases, such as chloride and fluoride, while appropriately positioned aromatic side arms can provide the countercation, TMA in these cases, with a suitable binding site which avoids the need of ion-pair dissociation. This interaction model is well confirmed, especially when the molecular ternary complex unit is highlighted. The crystal structures of the complexes **1**−**4**, and **7** with (TMA)Cl and **7-**(TMA)F, all show a quasi-identical conformation of the hosts and the ion-pair guests (Figure 1). The U atom displays a characteristic pentagonal bipyramidal 7-coordinate geometry, where the two uranyl's oxygens occupy the axial positions, while the tetradentate N_2O_2 frame of the salophen ligand encircles the uranium on the equatorial plane. The anion (Cl^- or F^-) completes the coordination sphere filling

(9) Hooft, R. W. *COLLECT*; Nonius BV: Delft, The Netherlands, 1998.
(10) Otwinowski, Z.; Minor, W. *Methods Enzymol.* **1997**, *276*, 307–326.
(11) Altomare, A.; Burla, M. C.; Cavalli, M.; Cascarano, G. L.; Giacovazzo, C.; Gagliardi, A.; Moliterni, A. G. G.; Polidori, G.; Spagna, R. *J. Appl. Crystallogr.* **1999**, *32*, 115–119.
(12) Farrugia, L. J. *J. Appl. Crystallogr.* **1999**, *32*, 837–838.
(13) (a) Sheldrick, G. M. *SHELXL-97*; Institüt für Anorganische Chemie der Universität Göttingen: Göttingen, Germany, 1998. (b) Sheldrick, G. M. *Acta Cryst.* **2008**, *A64*, 112−122.
(14) Sheldrick, G. M. *SADABS 2002/2008*; University of Göttingen: Göttingen, Germany, 2002/2008.
(15) Arnecke, R.; Böhmer, V.; Cacciapaglia, R.; Dalla Cort, A.; Mandolini, L. *Tetrahedron* **1997**, *53*, 4901–4908.

Table 1. Crystallographic Data for **3**-(TMA)Cl, **4**-(TMA)Cl, **7**-(TMA)Cl, **7**-(TMA)F, **6**, and **8**

	crystal					
	3-(TMA)Cl	**4**-(TMA)Cl	**7**-(TMA)Cl	**7**-(TMA)F	**6**	**8**
formula	$(C_{34}H_{24}N_2O_6Br_2U)$ $(C_4H_{12}NCl)\cdot 1/8\ H_2O$	$3(C_{36}H_{30}N_2O_6U)$ $4(C_4H_{12}NCl)\ 3CHCl_3$	$C_{72}H_{72}Cl_2N_6O_{12}S_2U_2$	$C_{32}H_{24}FN_2O_6$ SU, $C_4H_{12}N$	$C_{34}H_{24}N_4O_{10}$ U $2C_3H_6O$	$2(C_{34}H_{40}N_2O_7U)$, $2.25C_2H_3N$, $2H_2O$
space group	$I\bar{4}$	$I\bar{4}3d$	$I\bar{4}$	$I\bar{4}$	*Pnma*	$P21/c$
a [Å]	19.6629(2)	37.759(4)	18.9226(2)	18.9641(4)	9.4873(3)	26.1430(5)
b [Å]	19.6629(2)	37.759(4)	18.9226(2)	18.9641(4)	16.9434(7)	14.6744(2)
c [Å]	19.5797(4)	37.759(4)	19.5451(4)	19.0964(3)	23.8591(6)	18.7730(3)
α [deg]	90	90	90	90	90	90
β [deg]	90	90	90	90	90	90.300(1)
γ [deg]	90	90	90	90	90	90
V [Å^3]	7570.1(3)	53835(23)	6998.4(2)	6867.8(2)	3835.3(2)	7201.8(2)
Z	8	16	4	8	4	4
T [K]	173.0(1)	173.0(1)	123.0(1)	123.0(1)	123.0(1)	123.0(1)
D_{calc}	1.870	1.661	1.732	1.733	1.737	1.643
μ [mm^{-1}]	6.518	3.930	4.824	4.843	4.302	4.562
θ max [deg]	24.70	25.71	25	25	25.03	25
Θ comp.[%]	100	99.1	99.7	100	99.8	99.9
no. reflns.	6424	8413	6060	6065	3516	12673
no. param. restrains	466	546	433	397	282	887
	0	20	0	0	85	134
R1 [$I > 2\sigma(I)$]	0.030	0.0526	0.0301	0.0323	0.0437	0.0537
wR2 [$I > 2\sigma(I)$]	0.056	0.1063	0.059	0.0582	0.0869	0.0964
GOF	1.053	1.061	0.989	1.026	1.056	1.040
Flack param.	−0.015(6)	−0.007(9)	0.037(6)	0.026(6)	-	-

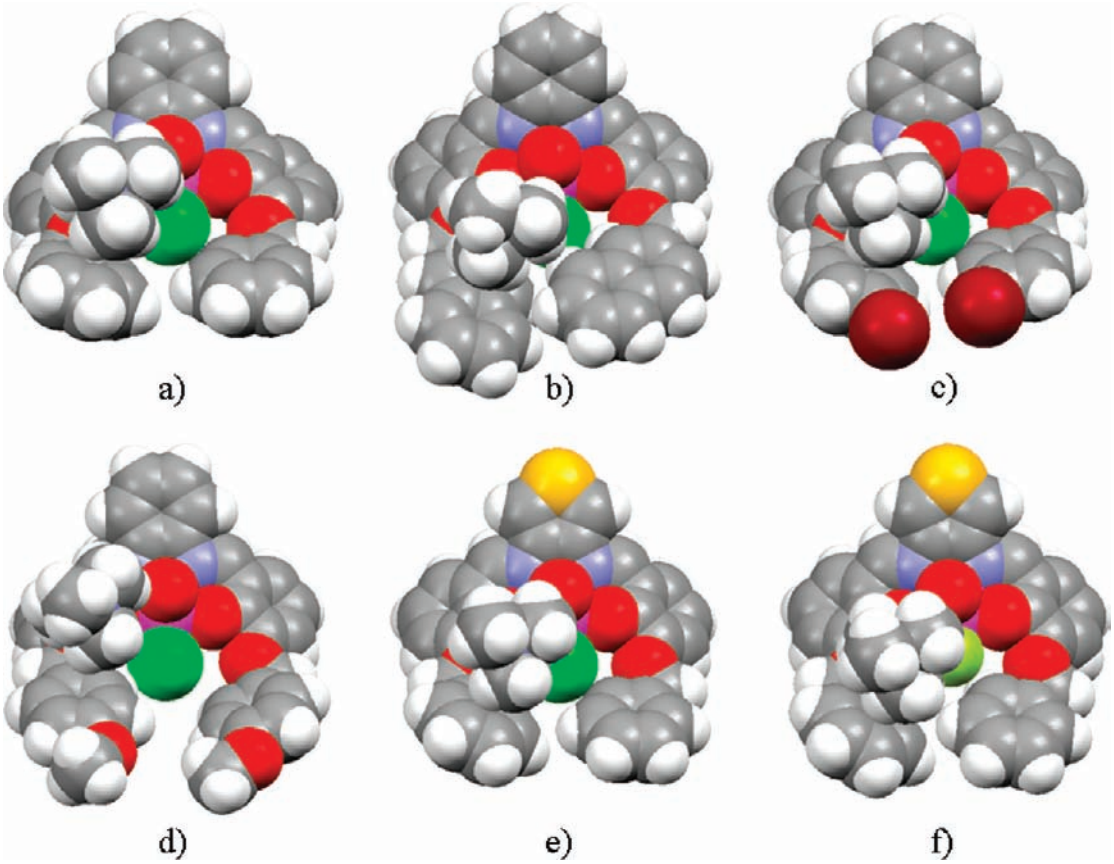

Figure 1. vdW presentations of the X-ray structures of the ternary (TMA)Cl complexes with **1** (a), **2** (b), **3** (c), **4** (d), and **7** (e) and the **7**-(TMA)F complex (f). Color codes: C = gray, H = white, N = blue, O = red, S = gold, Cl = green, Br = dark red and F = greenish-yellow, U = purple.

the fifth equatorial position (see the Supporting Information, Figure 1S). Anions are strongly bound to the UO_2-center, with distances in the range of 2.71−2.75 Å for Cl^- and 2.17 Å for F^-, respectively. The TMA cation maintains a strong electrostatic interaction with the anion, although weakened because of the reduced effective charge on the anion itself caused by the UO_2-coordination, which keeps the ion pair in contact. In addition, the TMA cation establishes a series of interactions with the surrounding, including $CH\cdots X^-$ (X = Cl, F), $CH\cdots O$, and cation-π interactions. If we look

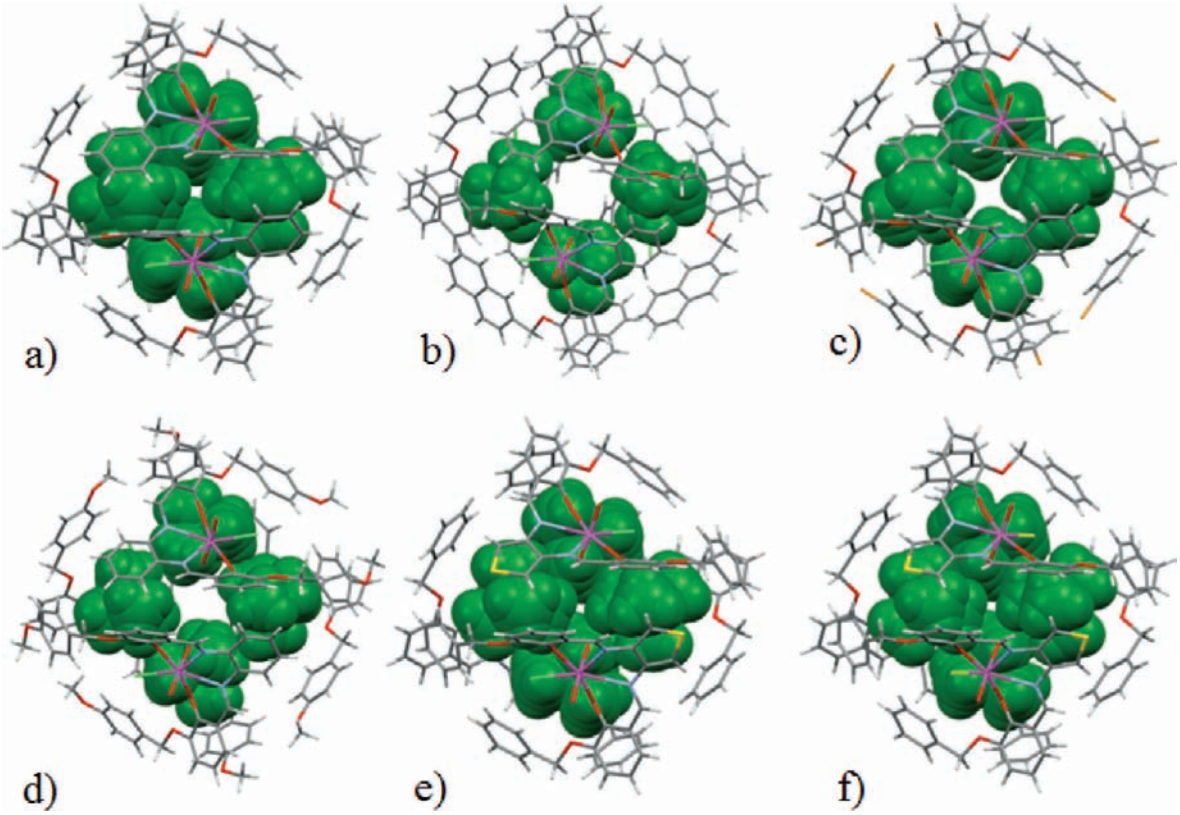

Figure 2. Capped-stick presentation of the receptor shell and the vdW presentation of the cation cluster (in dark green) for the complex with **1** (a), **2** (b), **3** (c), **4** (d), and **7** (e) with (TMA)Cl and the **7**-(TMA)F complex (f). Encapsulated and disordered solvent molecules were removed from **2**-(TMA)Cl, **3**-(TMA)Cl, and **4**-(TMA)Cl for clarity. Color codes: C = gray, H = white, N = blue, O = red, S = yellow, Cl = light green, Br = gold, and F = greenish-yellow, U = purple.

beyond the molecular units and focus on how such single units are arranged with respect to each other in the solid state, we discover that tetrameric, roughly ball-shaped 4:4 assemblies are formed. Through $CH\cdots Cl^-/F^-$ interactions the TMA cations are connected into clusters of four, situated inside the shell formed by the four receptors and shaped as isosceles tetrahedrons of various dimensions, depending on the receptor's structure. With the exception of the tetrameric assemblies of (TMA)Cl with receptors **2** and **4**, which crystallize in the trigonal $R3c$ and cubic $I\bar{4}3d$ space groups, respectively (vide infra), all the others structures respond to the tetragonal symmetry of the tetrameric units by crystallizing into tetragonal space group $I\bar{4}$.

Therefore, as mentioned before, the overall structure of the assembly consists of an ion-cluster, composed of four TMA cations, tightly encapsulated by a shell made of four receptor molecules with UO_2-bound Cl^- (or F^-) anions. Such tetrameric assemblies for the complexes of **1**−**4** and **7** with (TMA)Cl and for **7** with (TMA)F are shown in Figure 2, where the enclosing of TMA cations are more evidently displayed, and in Figure 3, where the complete assemblies vdW presentation are shown (See also the Supporting Information, Figure 2S). The placement of each TMA cation into the ball-shaped tetramer is such that multiple interactions of varying nature between the cation and both the receptors and the anions can be observed. For example, in the crystal structure of the **3**-(TMA)Cl, the TMA cation establishes (i) cation-π interactions with three adjacent aromatic rings; (ii) $CH\cdots Cl^-$ interactions with two of the four UO_2-bound anions; (iii) three $CH\cdots O$ interactions with three oxygens belonging to the receptor's frame. In this particular case, amid the $(TMA)_4$ unit a water molecule (disordered over two positions) is inserted (Figure 2c), displaying contact distances with one methyl of each TMA cation ($CH\cdots OH_2$ distance of 2.83 Å) and a weak hydrogen bond with the uranyl's oxygens ($H_2O\cdots O{=}U$ 2.77 Å).

A similar pattern of interactions is present in all the structures here reported, and it constitutes the driving force for the assemblies' formation. Table 2 lists the contact distances involving the TMA cation for complexes **1**− **4** and **7** with (TMA)Cl and for **7**-(TMA)F, together with other relevant structural data.

The role of the anion's identity (fluoride vs chloride) can be deduced by the comparison between **7**-(TMA)Cl and **7**-(TMA)F complexes (See also the Supporting Information, Figure 2S). As seen in Table 2, the nature of the anion does not significantly influence the cation-π interactions, whereas, as the donor ability of the F^--bound uranyl oxygens is strongly increased with respect to the Cl^- complex, stronger (and ca. 0.2 Å shorter) H-bonds with the polarized TMA methyl hydrogens are observed. The lower affinity of the UO_2 center toward larger and softer anions, such as Br^- and I^-,[8c] prevented the isolation of the corresponding (TMA)Br and (TMA)I complexes.

Calculating the volumes of the cavities delimited by the shell of receptor molecules and the volume of the TMAs cluster can reveal interesting information about the assemblies, the intramolecular interactions which are responsible for their formation, and in particular on how their size reflect the changes in the receptor structure. While the position of

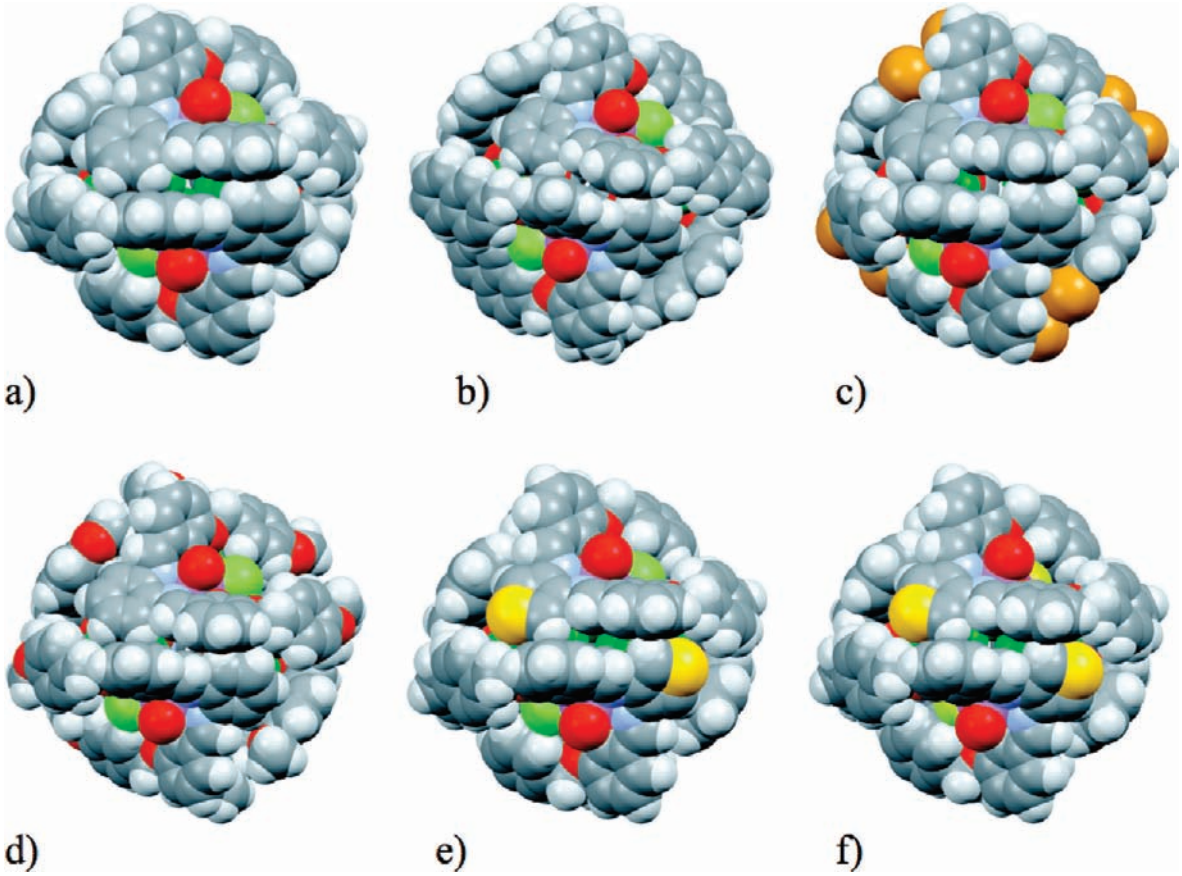

Figure 3. vdW presentation of the (TMA)Cl complex with **1** (a), **2** (b), **3** (c), **4** (d), and **7** (e) and the **7**-(TMA)F complex (f). Color codes: C = gray, H = white, N = blue, O = red, S = yellow, Cl = light green, Br = gold, F = greenish-yellow, U = purple.

the anion is directly related to overall dimension of the receptor (anions are bound to the UO_2-center by strong coordinative bonds), the cluster of four cations, which are more loosely interacting, is more independent from the receptor structure and may adapt its shape and its dimension to the size of the cavity. By varying the substituent R (Scheme 1) from the small R = H (**1**) to R = Br (**3**), R = OMe (**4**), and to naphthyl side arms in **2**, the cavity volumes increase, following the receptor's altered dimensions (Figure 1). The calculated estimates for the cavity volumes[16] for complexes of **1**−**4** with (TMA)Cl are 570, 691, 623, and 597 Å^3. Not surprisingly, the small receptor **1** generates the assembly which features the smallest cavity (570 Å^3), while **2**, the receptor bearing the bulkiest side arms, forms the assembly with the largest cavity (691 Å^3). Thus, significant changes, up to a 21% volume difference, are induced by structural changes in the receptor's unit.

The anion's identity also exerts an effect on the internal volume of the assembly, as seen by the comparison between **7**-(TMA)Cl and **7**-(TMA)F. The former displays a volume essentially identical to the one of **1**-(TMA)Cl, 570 Å^3, while the volume of the latter shrinks to 544 Å^3 because of the smaller size, and stronger electrostatic interactions of F^-. As far as the encapsulated TMA cations are concerned, which are the common structural units in the whole set of structures, the change in the cavity volume is reflected in their separation one from the others within the cluster.

As mentioned above, the TMA's nitrogens are located at the vertices of isosceles tetrahedrons, described by a set of two N···N distances, whose averaged values, for the various complexes, are the following: 5.8/6.8 (**1**-(TMA)Cl), 6.3/8.2 (**2**-(TMA)Cl), 6.0/7.5 (**3**-(TMA)Cl), 6.1/7.5 (**4**-(TMA)Cl), 5.8/6.7 (**7**-(TMA)Cl) and 5.7/6.7 Å (**7**-(TMA)F). Clearly, altering the dimensions of the receptor structure induces changes in the structure of the cation cluster. If the volumes of such tetrahedrons are calculated,[17] it is possible to note that they suffer only moderate variations in volume, up to about 10%, while their shape changes and may significantly flatten, for example in **2**-(TMA)Cl. This clearly indicates that, in spite of the necessity of maintaing a compact ion cluster inside the ball-shaped aggregates, the external shell of receptors is quite adaptable, and even with a 27% volume change of the cavity (691 Å^3/544 Å^3), the characteristic ball-shape is kept. In cases where the cavity is small, namely, **1**-(TMA)Cl, **7**-(TMA)Cl, and **7**-(TMA)F, the cations are packed tightly (Figure 2), nearly in vdW contact between each other. This is not always the case. In **3**-(TMA)Cl the

(16) The cavity size can be obtained from the crystal structure by removing the cation cluster from the tetrameric assembly and then calculating the void volumes of the crystal lattice with the PLATON VOIDS module. Such calculation gives the cavity volume of 572 Å^3 for **7**·(TMA)Cl. A simpler way to estimate the same volume is to measure the distance from the centroid of the cavity (defined as the centroid of the four halide anions) to the uranyl atom(s) and to calculate the volume of the resulting sphere as $V = 4/3\pi r^3$, where r is the distance between the cavity centroid and the uranium atom(s). The calculation made this way give for **7**·(TMA)Cl a volume of 570 Å^3, essentially the same as obtained from the crystallographic data. Therefore this second method has been considered as appropriate as the former, and it has used to calculate all the other volumes.

(17) Uspensky, J. V. *Theory of Equations*; McGraw-Hill Book Company, Inc.: New York, 1948.

Table 2. Selected Contact Distances (Å) for the Salophen-UO_2 Complexes **1**–**4**, **7**, and (TMA)X (X = Cl, F)

	type of interaction				
complex	cation-π	weak H-bond $N-H_2CH\cdots O$-R	weak H-bond $^{+}N-CH_3\cdots O{=}U$	Lewis acid−base $X^{-}\cdots UO_2$	weak H-bond $X^{-}\cdots H_3C-N^{+}$	miscellaneous interaction
1-(TMA)Cl	C41···c(C1−C6) 3.42 C40···c(C17−C21) 3.67 C42···c(C33−C38) 3.64	C40···O10 3.16	C43···O2 3.54	U1···Cl1 2.71	C43···Cl 3.68 C42···Cl 3.85	
2-(TMA)Cl	C54C···c(C37−39,C44−46) 3.38	C53C···O35B 3.33 C53C···O30B 3.36	C53···O1B 3.36	U1···Cl1 2.73	C53C···Cl1 3.62	O2···C91B (MeCN) 2.86
	C52E···c(C29B- C35B) 3.42	C53···O10B 3.34				O2···C92B (MeCN) 3.34
3-(TMA)Cl	C54···c(C1−C6) 3.57		C53···O10 3.44		C54···Cl 3.79	$wH_2O\cdots O10$ 2.77
	C53···c(C33−C38) 3.65	C54···O26 3.28	C53···O15 3.55	U1···Cl1 2.72		
	C52···c(C17−C22) 3.84				C52···Cl 3.76	$wH_2O\cdots C51$ 2.83
4-(TMA)Cl	C53B···c(C1−C6) 3.56	C51B···O10 3.45				
	C51A···c(C27−C32) 3.39	C51B···O15 3.41	C52B···O100 3.35	U1···Cl1 2.74	C52B···Cl3 3.67	$Cl_3CH\cdots Cl$ 3.44
	C54B···c(C35−C40) 3.52	C53B···O28 3.14	C51A···O200 3.55			
		C53B···O33 3.58				
7-(TMA)Cl	C53 ··· c(C33−38) 3.57	C52···O10 3.19				
	C53···c(C17−C22) 3.56	C52···O15 3.36	C51···O2 3.56	U1···Cl1 2.70	C51···Cl1 3.69	
		C54···O26 3.50				
	C52···c(C1−C4, S4) 3.48	C54···O31 3.24				
7-(TMA)F	C53···c(C33−C38) 3.50	C54 ···O26				
	C52 ···c(C17−C22) 3.56	3.16 C54···O31 3.33	C51 ··· O2 3.66, 3.67, 3.40	U1···F1 2.17	C53 ··· F1 3.46	
	C39 ···c(C1−C4, S4) 3.50	C53 ···O10 3.36			C51··· F1 3.32	
		C53···O15 3.44				

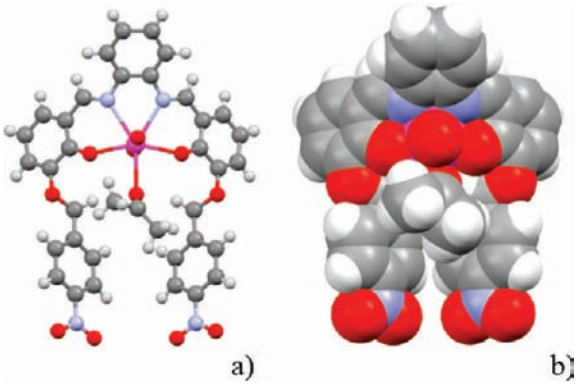

Figure 4. Ball and stick (a) and CPK (b) presentations of the receptor **6** (only one orientation of the disorder of the coordinated acetone is shown, the second acetone solvent molecule is excluded for clarity).

inner cluster allows a water molecule (disordered over two sites) to fit in, while in **2**-(TMA)Cl, the MeCN solvent molecules (also disordered), present in the crystallization media, are included into the center of the ion cluster. Moreover, both **2**-(TMA)Cl and **4**-(TMA)Cl display unbound (TMA)Cl ion pairs, which fill the voids within the lattice. Also, these two structures belong to NSC space groups (*R*3*c* and $I\bar{4}3d$). The change from $I\bar{4}$ to trigonal *R*3*c* and cubic $I\bar{4}3d$ results from the trigonal nature of the unbound and solvated TMACl ion pair situated on a 3-fold symmetry axis. It is plausible to consider that having bulky side arms may render the packing less efficient, with the consequence of the inclusion of additional molecules in the lattice.

More interestingly, *R*3*c* is a truly polar space group, hence **2**-(TMA)Cl represents a even more exceptional case. Polar materials not only may produce piezoelectricity, as all NCS material, but they may possess a non-null macroscopic dipolar moment ($\boldsymbol{P} \neq 0$) defined on an exclusive direction in the crystal lattice (defined polar axis in crystallographic terms). This feature extends the material properties to pyroelectricity. In this respect, materials which linger on the boundary between the organic and inorganic domains, as those presented here, may have advantages over purely inorganic, or purely organic materials.

Unfortunately, we were not able to obtain a single crystal for the (TMA)Cl or (TMA)F complex with receptor **5**, nor with **6**. In the latter case, such failure is probably due to the effect of the substitution (R = NO_2), which by reducing the electron density on the side arms lowers the affinity for the ion pair binding.[18] The reduced solubility of the receptor itself led to difficulties in the crystallization attempts with TMA salts in $CHCl_3$. However, receptor **6** crystallized as a solvate from an acetone solution, and its X-ray structure is presented in Figure 4. When crystallized with no (TMA)Cl present, no higher order assemblies are formed. Notably, the crystal lattice is stabilized by $C_{(arom)}$-H···O_2N- interactions.

The six ball-shaped tetrameric assemblies described above, and formed upon crystallization, present an arrangement which seems to be quite general, and extremely favored in the solid state for this type of salophen-UO_2 complexes when co-crystallized with TMA halides salts. Most interestingly, the presence of the NCS lattice is also a feature common to all of these structures. As an example, Figure 5 shows the crystal packing of the tetrameric ball-shaped units for **3**-(TMA)Cl.

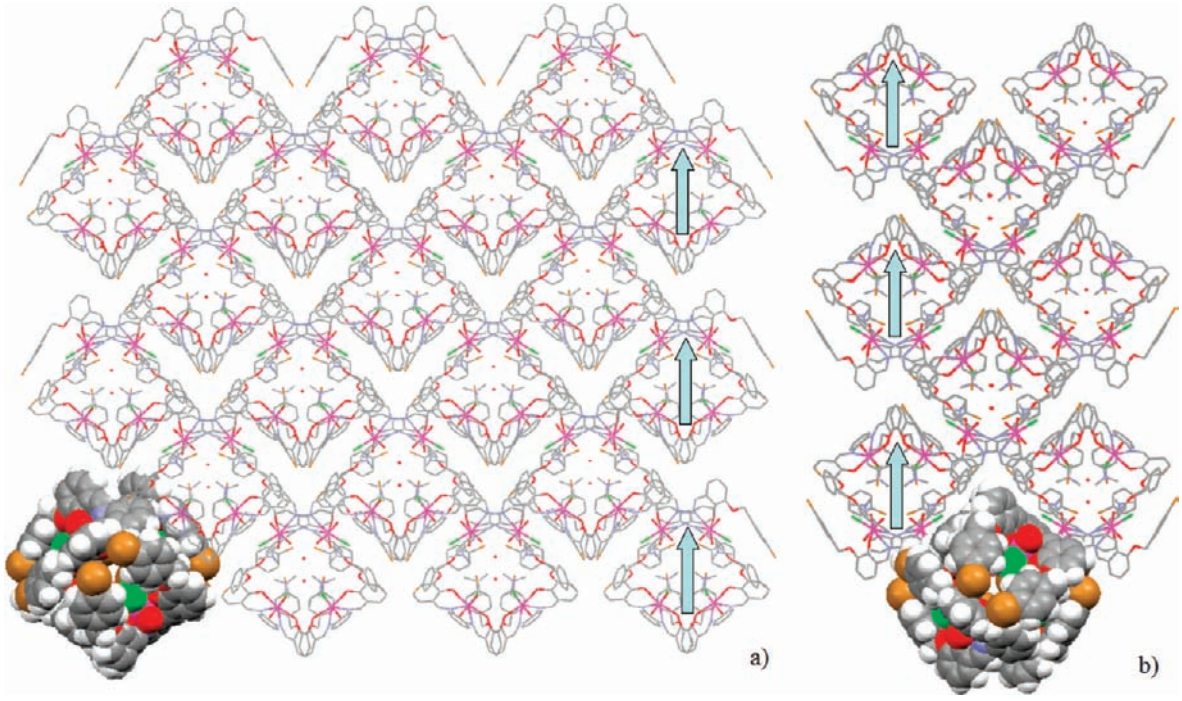

Figure 5. Orientation of the tetrameric ball-shaped aggregates (wireframe presentation) in the crystal lattice of **3**-(TMA)Cl. Two views, along the *a*-axis (a) and along the *b*-axis (b), are shown. The turquoise arrows represent the direction of the alignment. One ball-shaped aggregate is shown in vdW presentation.

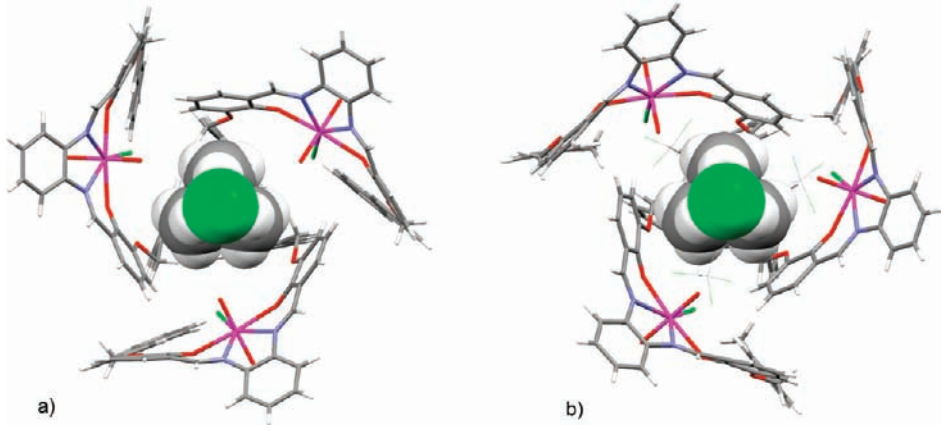

Figure 6. Spatial arrangements of tetrameric ball shaped aggregates in the surrounding of the unbound (TMA)Cl ion pair (in vdW presentation) in the complexes of (a) **2**-(TMA)Cl, and (b) **4**-(TMA)Cl along the 3-fold axis.

As it is clearly seen, the ball-shaped assemblies are all arranged with the same orientation in the crystal lattice and no inversion center is present. Almost identical arrangements are also found for **1**- and **7**-(TMA)Cl and for **7**-(TMA)F. Notably, strong CH$\cdots\pi$ interactions take place in between the tetrameric shell units, which definitely contribute in further stabilizing the assemblies (shortest CH$\cdots\pi$ distances in **1**- and **7**-(TMA)Cl of 2.74 and 2.65 Å, respectively, while distances in **7**-(TMA)F are 2.76 Å).

As mentioned earlier, the space groups of **2**- and **4**-(TMA)-Cl are different from the rest of the complexes. In fact, in these two cases, unbound (TMA)Cl ion-pairs are also constituents of the lattice as they organize themselves between three tetramer units, thus introducing a 3-fold symmetry element in the structure. This is clearly depicted in Figure 6 where the TMA cation is shown to interact with three adjacent salophen-UO_2 receptors via cation-π interactions. Therefore, such forces not only appear to have a strong influence on the formation process of the tetramer, but also in directing the lattice architecture. It must be remembered that in all cases, an excess of the TMA salts was present in the crystallization mixture to favor the host−guest formation.

These findings indicate that, in these systems, the NCS, and in one case, polar lattices are not achievable only by a specific alignment of the tetrameric ball-shaped tetramers, and therefore might be related with the intrinsic nature of the salophen-UO_2 complexes.

As said before, although being not well understood, the formation of NCS crystals is not rare a phenomenon, and a CSD[19] search reveals a number of macrocyclic or N/O

(18) Unpublished results show how the substitution on the receptors' sidearms with electron withdrawing groups lowers the affinity for (TMA)Cl salt.

Scheme 3. Molecular Formulae of Salen- and Salophen-UO_2 Complexes, and Other UO_2-Complexes Whose Polar Crystal Structures Are Reported in the Literature[a]

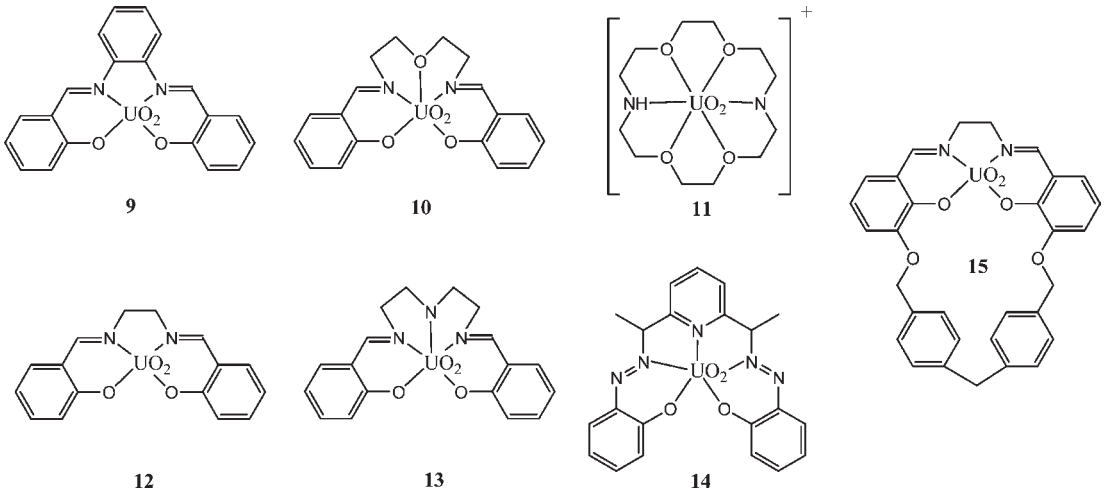

[a] **9**·MeCN (YALSOU); **9**·DMSO (NICQAS); **10** (SALOPV); **11**·$CF_3SO_3^-$ (YOWFOF); **12**·pyridine (NIPBUK); **13** (SOJKUX); **14**·pyridine (AYOJON); **15**·MeOH (JODXOQ).

tetra- and penta-dentate ligands which form UO_2-complexes and that are reported to crystallize in polar space groups (see Scheme 3). For example, in the crystal structures of the complexes **9**·MeCN (*Ccm*21), **9**·DMSO (*P*21), **12**·pyridine (*Pca*21), and **14**·pyridine (*Fdd*2) (where the fifth equatorial site of the UO_2 center is occupied by coordinated MeCN, DMSO, or pyridine solvent molecules),[8b,20] the molecular entities are positioned in such a way to have all the U···$N_{(MeCN,\ pyridine)}$, or U···$O_{(DMSO)}$ vectors parallel (or almost) to each other. Worth noting, as an example which illustrates the difficulty in predicting the occurrence of NCS packing, is the case of **14**·DMSO, which, contrary to its pyridine analogue, crystallizes in a centrosymmetric space group (*Pnma*).[21]

Molecules **10** (*Ccm*21) and **13** (*Pca*21) also crystallize in NCS and polar space groups, this time, by orienting the molecular concavity facing to one single direction. Although in a less evident way, also molecules **11** (*Ccm*21) and **15** (*P*1) crystallize into lattices with no center of inversion. In all case, the repeating unit in the crystal architecture consists of the molecular unit, or of its solvate, and no aggregates or adducts of higher complexity are found.

Indeed, these systems significantly differ, in terms of complexity of the lattice architecture, from the structures described in this work. The latter crystal structures show no evident alignment of single molecular units, whereas globular, tetrameric ball-shaped aggregates are found. In light of a hierarchical view,[22] we can speculate that the organization of the molecular components in NCS crystal lattices must be induced at a certain stage in the crystal formation process. As pointed out by Mandolini et al., non-symmetrically substituted Salophen-UO_2 complexes bear an intrinsic chirality,[23] because of their curved structural frame. Although the UO_2-complexes in Scheme 1 are symmetric, their isolated ternary adducts formed by interaction with the ion pair, as presented in Figure 1, are asymmetric in nature. In solution, this intrinsically asymmetric conformation would be in equilibrium with its equivalent mirror image, simply obtainable by exchanging the interacting side arm, and furthermore by the flipping mode of the salophen-UO_2 frame.[23] In the solid state, and in the crystallization process, the situation could be different. Provided that a preferential interaction of TMA with one of the two side arms is actually occurring, and were the kinetics of this exchange between conformations is made kinetically slow, for instance, by the formation of stable intermediate aggregates, an intrinsically chiral object would be formed. The fact that the tetrameric ball shaped aggregates lack of a center of inversion is clearly in favor of this interpretation; however, that cannot be the only factor which determines the formation the observed structures.[24]

The validity of the above interpretation relies on the presence of a strong interaction which could favor the formation of a non-symmetric intermediate species as directing element for the formation of these crystal structures.

^{1}H NMR solution studies in $CHCl_3$ have already demonstrated that receptor **1** strongly associates to (TMA)Cl (K = 17600 M^{-1}) in a 1:1 fashion.[8a,c] Such affinity for TMA is severely reduced in the case of compound **8** (Scheme 1 and 3), in which the aromatic side arms are replaced with aliphatic cyclohexyl moieties.

As demonstrated by the titration plot in Figure 7, which shows the δ upfield shift of the TMA signals upon increase of

(19) *Cambridge Structural Database* (version 5.29, the AUG 2008 update, 456628 X-ray crystal structures); The Cambridge Crystallographic Data Centre: Cambridge, U.K., 2008.

(20) Takao, K.; Ikeda, Y. *Inorg. Chem.* **2007**, *46*, 1550–1562. Bharara, M. S.; Tonsk, S. A.; Gorden, A. E. V. *Chem. Commun.* **2007**, 4006–4008. Gatto, C. C.; Lang, E. S.; Kupfer, A.; Hagenbach, A.; Wille, D.; Abram, U. *Z. Anorg. Allg. Chem.* **2004**, *630*, 735–741.

(21) Gatto, C. C.; Lang, E. S.; Jagst, A.; Abram, U. *Inorg. Chim. Acta* **2004**, *357*, 4405.

(22) Elemans, J. A. A. W.; Rowan, A. E.; Nolte, R. J. M. *J. Mater. Chem.* **2003**, *13*, 2661–2670. Yan, Y.; Huang, J. *Coord. Chem. Rev.* **2010**, *254*, 1072–1080. Yang, Y.; Wang, C. *Chem. Soc. Rev.* **2009**, *38*, 2576–2589. Kresge, C. T. *Adv. Mater.* **2004**, *8*, 181–182.

(23) Dalla Cort, A.; Mandolini, L.; Palmieri, G.; Pasquini, C.; Schiaffino, L. *Chem. Commun.* **2003**, 2178–2179.

(24) Alkali metal halides complexes with salophen-UO_2 have been reported (see ref 8b). The dimeric assemblies which they feature are centrosymmetric; hence, they do not crystallize in polar space groups. We speculate that the stepwise formation of a tetrameric species (monomer-, dimer-, trimer-, tetramer) intrinsically involves non centrosymmetric species (trimer), while this not the case for dimeric species like the alkali metal complexes.

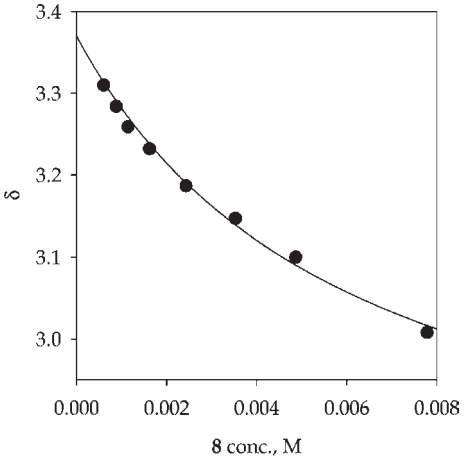

Figure 7. ^{1}H NMR titration plot of (TMA)Cl with receptor **8**, in $CDCl_3$ at 25 °C.

the complex **8** concentration, the phenyl to cyclohexyl substitution significantly affects the affinity, and the association constant drops to about 130 M^{-1}. Receptor **8** can be considered an improved model with respect to **9**, employed in previous investigations (Scheme 3),[8a,c] as it takes better into consideration the steric contribution of the two side arms, especially in relation to the position that TMA must adopt to maximize the electrostatic interaction with the UO_2-bound anionic species (which always remains the driving force for the association with the cation). The fact that receptor **8** is found to bind much less efficiently than **9**, suggests a more critical role of the cation-π interactions established between the TMA and the aromatic side arms of these receptors than previously attributed.

This finding also easily explains the fact that all the crystallization attempts made to obtain the (TMA)Cl complex with **8** in the solid state failed, and that only the solvated receptor was successfully crystallized. The X-ray determined structure of compound **8** is shown in Figure 8. It shows some interesting features, as the UO_2-complexes assemble in dimeric structures which incorporate four water molecules, two of them bound to the UO_2 center, while the other two interact via H-bonds. This situation has definitely a strong resemblance with dimeric alkali metal salts complexes previously observed by us.[8b]

If cation-π interactions can therefore be considered relevant for the assembly formation as observed in the crystalline state, other intermolecular forces may also be responsible for the occurrence of metastable intermediates which could represent the directing unit in the crystal formation. Mass spectroscopy have been extensively used for seeking species which can be elusive and present in low concentration in solution under certain conditions, (for example, at the beginning of the crystallization process), but whose detection can be accomplished under gas-phase conditions using ESI mass spectrometry.[25]

We explored the possibility of the occurrence of receptor-(TMA)Cl aggregates of various composition by ESI experiments, and at the same time, we compared the behavior of receptor **1** to that of the novel reference compound **8**.

(25) Miras, H. N.; Wilson, E. F.; Cronin, L. *Chem. Commun.* **2009**, 1297–1311. Zhu, H.-F.; Kong, L.-Y.; Okamura, T.-a.; Fan, J.; Sun, W.-Y.; Ueyama, N. *Eur. J. Inorg. Chem.* **2004**, *7*, 1465–1473. Schalley, C. A. *Mass Spectrom. Rev.* **2002**, *20*, 253–309. Schalley, C. A. *Int. J. Mass Spectrom.* **2000**, *194*, 11–39.

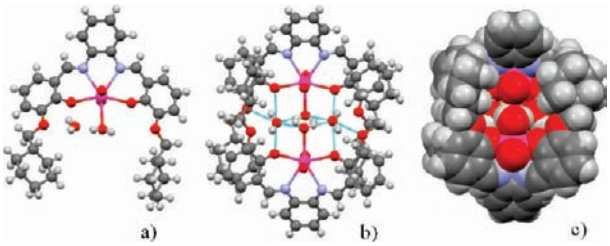

Figure 8. View of the receptor **8** (a) and its water-assisted dimer in ball and stick (b) and vdW model (c).

When a mixture of **1** (1×10^{-5} M) and (TMA)Cl (5×10^{-5} M) were sprayed, peaks of composition $[\mathbf{1}\cdot(TMA)_2Cl]^+$ (main peak), $[\mathbf{1}\cdot(TMA)]^+$, and $[\mathbf{1}_2\cdot(TMA)]^+$ were observed in the mass spectrum. No significant peaks suggesting higher order aggregates, more closely resembling to the ball-shaped tetramers, were visible. A 2×10^{-5} M solution of receptors **1** and **8** containing 0.5 equiv of (TMA)Cl was also spayed in $CHCl_3$ inducing a competition between the two receptors for the ion-pair guest. The peaks of composition $[\mathbf{1}\cdot(TMA)_2Cl]^+$ (main peak) and $[\mathbf{8}\cdot(TMA)_2Cl)]^+$ were found in a 2:1 ratio, an indication for a little preference of (TMA)Cl for receptor **1** over complex **8**, under the ESI-mass experiment conditions. Other relevant peaks were observed for $[\mathbf{1}_2\cdot(TMA)]^+$, $[\mathbf{8}_2\cdot(TMA)]^+$, and $[\mathbf{1}\cdot\mathbf{8}\cdot(TMA)]^+$ with no relevant difference in peak intensity between the former two, but with an evident preference for the latter hetero species $[\mathbf{1}\cdot\mathbf{8}\cdot(TMA)]^+$. Under these conditions, the specific cation-π interactions are apparently much less significant, and electrostatic and vdW interactions dominate. No peaks which could be considered as the presence of higher aggregates of specific composition could be found. These findings indicate that in the circumstances under which the crystallizations occur, the high concentration, the cation-π interactions which were found determinant in solution phase, and the strong CH$\cdots\pi$ interactions which pack the tetrameric units into a ordered lattice, are all prominent for the formation of the assemblies described in this work.

Conclusions

The lack of a center of symmetry in a crystalline lattice, or more stringently, the occurrence of polarity in crystallographic terms, are not rare events in crystal formation; this notwithstanding, the factors which induce such ordering of the molecular components are not always clear. In addition, the properties which result from the non-centrosymmetry, such as pyro-, ferro-, and piezo-electricity, are extremely interesting, and they are subject of extensive investigations for development of new functional materials.[1,2] In view of the strict necessity of a specific spatial organization for the obtainment of the desired properties, regardless of the molecular identity, it is highly valuable to explore any unusual aggregation motifs present, when leading to NCS and polar crystals, to acquire useful information which could eventually shed light into the mechanism of their formation.

Here, co-crystallization studies of TMA chlorides and fluorides with salophen-UO_2 complexes **1**−**7**, belonging to a well-established class of ion pair receptors, show that the occurrence of NCS crystal structures in their host−guest complexes is a quite general phenomenon. Ball-shaped tetramers composed of four ion-pairs amid a shell made of four receptors are the supramolecular units featured in the crystalline

lattice. Such assemblies are quite robust and adaptable as they may endure a certain degree of structural modification in their basic molecular components and still retain their overall shape, and an increase of up to about 27% in volume of the internal cavity of the receptor shell is indeed tolerated.

In the majority of the structures presented here, the ordering of the tetrameric ball-shaped aggregates results in NCS packing in tetragonal symmetry ($I\bar{4}$); however, in **2**- and **4**-(TMA)Cl different spatial arrangements are observed (space groups $R3c$ and $I\bar{4}3d$, respectively). In these two cases, each of the unbound (TMA)Cl ion pairs co-crystallized in the lattice fits itself in between three adjacent receptor shells, introducing an additional 3-fold symmetry element to the whole crystal structure. These findings indicate that the NCS arrangements and polarity are not necessarily achieved by the alignment of the ball-shaped tetramers, as originally thought, but must reside in the asymmetric nature of the tetrameric aggregates themselves. The intrinsic chirality of asymmetric [salophen-UO_2−$(TMA)_x(Cl)_y$] adducts which may form during the crystallization process could exert an influence on establishing the observed non-centrosymmetry of the lattice. In addition, the **2**-(TMA)Cl structure is polar; thus, it may possess a macroscopic dipole moment which extends the range of possible applications in the field of functional materials. This feature makes these materials intriguing and worth to be explored in more detail. In this respect, ^{1}H NMR and ESI-mass studies were undertaken to extrapolate from solution- and gas-phase behavior some additional information on the properties of the uranyl-salophen complexes and on the way they assemble into the crystalline arrangements observed. A novel reference compound, **8**, was synthesized to assess the specific contribution of cation-π interactions to the tetrameric assembly formation. ^{1}H NMR titrations experiments with **8**, which possesses aliphatic instead of aromatic side arms, attribute to cation-π interactions a more important role in the overall energy balance for the host−guest complexes formation in solution and, therefore, in the crystallization process. Instead, the search in the gas-phase of higher order aggregates failed, since only dimeric species are detected by ESI-mass experiments.

The results reported here broaden the interest on salophen-UO_2 complexes by showing that NCS crystalline solids can be obtained from their host−guest complexes, thus expanding their field of applications to the domains of material chemistry. Indeed, piezo- and pyro-electricity are attractive bulk properties of the material, which necessitate non-centrosymmetric and polar arrangement to emerge.

Further studies aimed at the inclusion of novel species amid the tetramer's cavity, for example, neutral and multicharged compounds having large dipole moment and hyperpolarizability, while maintaining the overall NCS and polar organization in the crystal lattice, are currently underway.

Acknowledgment. The financial support from the Academy of Finland (K.R., proj. no. 212588 and 218325; M.N. and E.N. proj. No. 116503) is gratefully acknowledged.

Supporting Information Available: CIF files for the structures of complexes **3**-, **4**-, and **7**-(TMA)Cl and for **7**-(TMA)F; CIF files for the structures of compounds **6** and **8** and Figures 1S and 2S. This material is available free of charge via the Internet at http://pubs.acs.org.